Avrupa Bilim ve Teknoloji Dergisi
Sayı 17, S. 823-832, Aralık 2019

Araştırma Makalesi

www.ejosat.com ISSN:2148-2683

European Journal of Science and Technology
No 17, pp. 823-832, December 2019

Research Article

The Effect of LED Deployment on RSSI-based VLP Systems

Yasin Çelik[1*]

[1] Department of Electrical-Electronics Engineering, Faculty of Engineering, Aksaray University, Aksaray, Turkey (ORCID: 0000-0001-8972-9970)

(First received 3 October 2019 and in final form 1 December 2019)

(**DOI:** 10.31590/ejosat.628709)

ATIF/REFERENCE: Çelik, Y. (2019). The Effect of LED Deployment on RSSI-based VLP Systems. *European Journal of Science and Technology*, (17), 823-832.

Abstract

In this paper, the effect of light emitting diode (LED) deployment is investigated based on the received signal strength indication (RSSI) technique for visible light positioning (VLP) systems. The optical code division multiple access (OCDMA) is used as a multiplexing technique to transmit the location and RSSI information of LEDs simultaneously. For different highly reflective indoor scenarios, LEDs are placed on the ceiling of a room considering homogeneous illumination. The illuminance of the room is provided particularly with 400 lux *minimally* at the desk height. In order to demonstrate the uniformity of lighting for different indoor scenarios, the uniformity illuminance ratio (UIR) values are also obtained in this study. In addition, electrical signal-to-noise ratio (SNR), an important parameter for reliable communication, is calculated at desk height for each scenario considered and an SNR level of 45 dB is obtained at a *minimum*. The simulation results demonstrate that the mean square error (MSE) of the estimated location is reduced with an increase in the number of visible access points (VAPs). The MSE of the distance for number of VAPs 12 and 16 are the best, however, the scenario with 16 VAPs is preferable with a better uniformity illuminance ratio (UIR) parameter. In terms of illuminance, all the cases have the average illuminance value more than 450 lux.

Keywords: Visible light positioning, RSSI, Trilateration, CDMA.

LED Dağılımının RSSI Tabanlı Görünür Işık Konum Belirleme Sistemleri Üzerindeki Etkisi

Öz

Bu çalışmada, ışık yayan diyot (LED) dağılımının alınan sinyal gücü göstergesi (ASGG) tabanlı görünür ışık konum belirleme sistemlerinin performansı üzerindeki etkisi incelenmiştir. LED'lerin konum ve ASGG bilgisini alıcı birime göndermek için optik kod bölmeli çoklu erişim tekniği çoğullama tekniği olarak kulllanılmıştır. Bina içi yansımanın kuvvetli olduğu senaryolar için LED'ler tavana homojen bir aydınlatma sağlayacak şekilde yerleştirilmiştir. Oda içindeki aydınlatma seviyesi masa yüksekliğinde *minimum* 400 lüks sağlanacak şekilde ayarlanmış ve aydınlatmanın homojenliğini farklı bina içi senaryolarda ortaya koymak için aydınlık homojenliği oranı (AHO) değerleri elde edilmiştir. Ek olarak, güvenli haberleşme için önemli bir parameter olan elektriksel sinyal gürültü oranı değerleri dikkate alınan her senaryo için fotodedektör (PD) düzleminde hesaplanmış ve *minimum* değer olarak 45 dB elde edilmiştir. Simulasyon sonuçları LED dizilerinin (VAP) sayısı arttıkça kestirilen konumun ortalama karesel hata (OKH) değerinin azaldığını göstermiştir. VAP sayısı 12 ve 16 olduğu durumda en iyi OKH değeri elde edilmiştir. Bununla birlikte AHO değeri daha iyi olan 16 VAP içeren senaryonun daha tercih edilebilir olduğu ortaya konmuştur. Aydınlatma açısından bakıldığında tüm senaryolarda ortalamada 450 lüks üzerinde aydınlık düzeyi sağlanmıştır.

Anahtar Kelimeler: Görünür ışık konum belirleme, RSSI, Trilaterasyon, CDMA.

[*] Corresponding Author: [1]Department of Electrical and Electronics Engineering, Faculty of Engineering, Aksaray University, Aksaray, Turkey, ORCID: 0000-0001-8972-9970, yasincelik@aksaray.edu.tr

1. Introduction

The Global Positioning System (GPS) is widely used in outdoor environments in order to provide positioning and navigation. In challenging environments, however, such as indoor environments, GPS is inefficient and discontinuous due to the degraded and interrupted signals transmitted by satellites. As an alternative, indoor positioning systems (IPS) using indoor wireless signals such as WiFi, Bluetooth, radio frequency identification (RFID) have been proposed to fulfill the drawbacks of GPS signals, though, such systems have lower positioning accuracy and high costs [1]. Furthermore, RF solutions are not convenient to be used in some environments such as healthcare facilities, highly flammable industrial environments, aeroplanes etc., due to sensitivity to electromagnetic interference (EMI). Besides, RF spectrum is intensively used for data transfer so there is no enough spectrum for other systems [2].

Recently, positioning systems based on light emitting diodes (LEDs) have become very popular where visible light signals are used instead of RF signals. An LED was previously known for its important features, some of which are high bandwidth and high speed wireless data transmission, energy-efficient technology, long lifetime with reliable illumination and cost-efficiency. Thanks to these properties, an LED can be used for illumination and positioning, *simultaneously*. Therefore, it is predictable that the novel indoor localization technology is based on visible light positioning (VLP) systems utilizing LEDs [3]-[8]. Besides, these systems provide more accurate results (0.1-0.35 m positioning error) when compared to WiFi (1-7 m), Bluetooth (2-5 m), RFID (≤2 m) [9].

In the positioning systems literature, several techniques are proposed to find the target position, which are time of arrival (ToA), time difference of arrival (TDoA), angle of arrival (AoA), and received signal strength indication (RSSI) [10]. Among these, the RSSI based distance measurement with trilateration algorithm is standing out due to simplicity and low-cost. However, in VLP, RSSI is generally applied with the special case: line-of-sight (LOS) link characteristics [11]-[15].

Since luminous fluxes from the LEDs are dispersed around the room and this creates reflecting (non-line-of-sight, NLOS) components from the walls, ceiling, and any other surfaces within the room, the NLOS link has a considerable contribution on the received light intensity. Thus, the reflecting components must be taken into account for the RSSI-based VLP systems because of their negative impact on system performance metrics. In [16], NLOS components up to three bounces are investigated for the systems mentioned and the distance error performances are obtained both for LOS and NLOS components in the whole room. In the study [17], the reflections of the indoor environment are taken into account and the received signals are simulated at harsh locations inside the room, e.g. corners and wall edges. Strong reflecting signals are detected and their impact on the positioning error is also investigated. In another study [18], a hybrid algorithm is used to select four strongest LED signals with multipath reflections for approximate coordinate estimation then, weighted centroid algorithm is introduced to detect position. In the work [19], the performance of RSSI-based VLP system with NLOS components is evaluated using the received optical power levels from LEDs under the condition of both noisy and noiseless channel. The accuracy of *10 cm* on average is achieved at an SNR value of greater than *12 dB*. However, all these studies are based on a single indoor configuration using *generally* four LEDs.

For a 2-D position estimation with trilateration algorithm, at least three LEDs should be used with known locations in the VLP scenario. As well as the average SNR on the detector plane, the individual SNR of each LED also determines the performance of the system [20]. Therefore, the minimum value of the individual SNR has to be maximized to achieve the best distance error performance. This is the main motivation of our study as we investigate the effect of LED deployment via considering various number of LEDs in the indoor scenario on the performance of RSSI based VLP system. Besides, the illumination is also considered for proper task lighting at the desk height. The main contribution of this paper is to present the relationship between the MSE of the distance and the number of VAPs placed on the ceiling.

2. Material and Method

2.1. System Model

In this study, an indoor VLP system using multiple visible access points (VAPs) as transmitters (Txs) and a single photo-detector (PD) as a receiver (Rx) is considered. To transmit different data from the VAPs in the same room, the Optical Code Division Multiple Access (OCDMA), which is easily realized by On-Off Keying (OOK) and Walsh codes, is used as the multiplexing technique [21]. In this technique, each VAP is mapped to a unique code to represent its identity and also position information. The DC bias signal is used to modify the bipolar codes to unipolar ones at the Tx side. Another DC signal, the turn-of-voltage (TOV), is subsequently added to unipolar OCDMA signal. Thus, the resulting electrical signal becomes suitable for driving the LEDs. The received electrical signal at the Rx side, y, is given by

$$y = \mathbf{hx} + n, \tag{1}$$

where **h** and **x** represents the $1 \times N_t$ channel gain vector and $N_t \times 1$ transmitted symbol vector, respectively. Here N_t denotes the number of VAPs, and n is the noise parameter. The total noise in the receiver is the sum of the shot noises and the thermal noise. The shot noise due to background radiation is the dominant one among the other shot noises reasoned from received signal and dark current. The thermal noise, which is modelled by the additive white Gaussian noise (AWGN) independent of the transmitted signal, however, is

always dominant in such systems. Therefore, we consider n as a zero mean Gaussian random variable with a variance of $\sigma^2 = N_0 / 2$ per dimension.

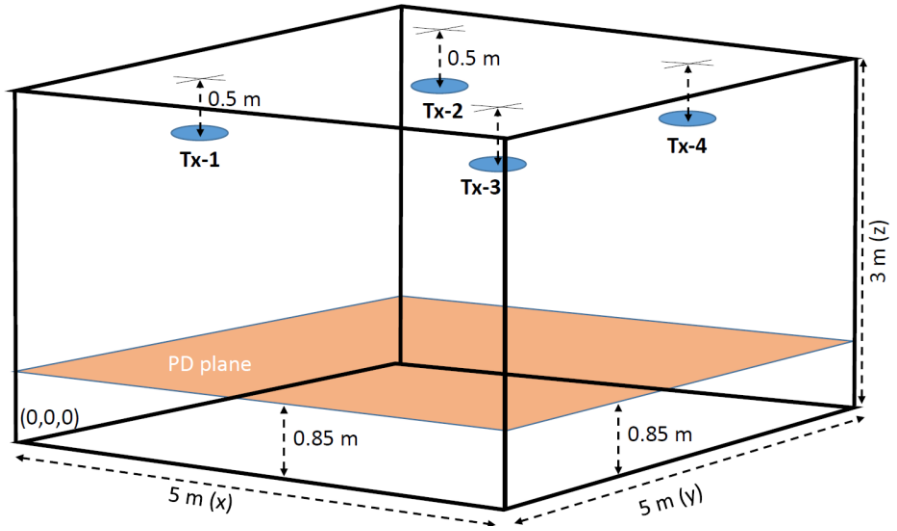

Figure 1. Indoor geometry for $N_t = 4$.

The transmitted signal from each LED in the i^{th} VAP, $x_i(t)$, is given by

$$x_i(t) = s_i(t) + \Delta + \Lambda, \tag{2}$$

where $s_i(t)$ corresponds to the OCDMA signal, Δ is the DC bias signal, and Λ is the TOV. The optical power emitted from each LED in the VAP, P_i^o, is obtained as

$$P_i^o = \frac{1}{T_c} \int_0^{T_c} x_i(t)\, dt, \tag{3}$$

where T_c is the chip period of the $s_i(t)$. Thus, P_i^o corresponds to the time average of $x_i(t)$, which is equal to the $\Delta + \Lambda$, since the $s_i(t)$ is inherently a zero mean signal over one chip period [21].

The DC part of the received signal is removed before the correlation operation so that the orthogonality between codes are remained. After decoding the CDMA signal, the VAP identification and also the RSSI information is determined for each VAP. The bit error ratio (BER) of 10^{-4} is achieved in the OCDMA up to 16 users with modified bipolar codes under the SNR of 15 dB. This BER value is sufficient enough to ensure reliable communication with error correcting codes [22]. In this study, it is shown that the SNR value is much higher than 15 dB in the whole room and perfect synchronization is assumed. Thus, the multiple access interference (MAI) is completely prevented. On the other hand, the VLP system uses low data rates so that the correlation bandwidth of the channel is larger than the bandwidth of the data signal. In Fig. 2, power delay profile (pdp) of the channel is shown for two different indoor scenarios and it is seen that the correlation bandwidth of the channel is larger than 50 MHz, which is much larger than the signal bandwidth. Therefore, inter-symbol interference (ISI) is not a problem encountered in this study, as well.

N_t circles are taken into account to determine the VAPs locations in the xy-plane, specifically, $z = 2.5$ m constant ceiling plane. To guarantee uniform illumination in the room and to obtain the best individual SNRs reasoned from each VAPs, it is ensured that N_t *imaginary* circles are placed in the ceiling plane with equal and also maximum diameter. Then, the centers of the circles are determined as the x and y positions of the VAPs. These positions for different number of VAPs are given in Table 1.

Table 1. x-y positions of VAPs.

N_t	***x-y positions (m)***
4	{1.25-1.25; 1.25-3.75; 3.75-1.25; 3.75-3.75}
5	{1.03-1.03; 3.96-1.03; 2.50-2.50; 1.03-3.96; 3.96-3.96}
8	{0.85-0.85; 4.14-0.85; 2.50-1.29; 1.29-2.50; 3.70-2.50; 2.50-3.70; 0.85-4.14; 4.14-4.14}
9	{0.83-0.83; 2.50-0.83; 4.16-0.83; 0.83-2.50; 2.50-2.50; 4.16-2.50; 0.83-4.16; 2.50-4.16; 4.16-4.16}
12	{0.70-0.70; 3.10-0.70; 1.90-1.46; 4.29-1.46; 0.70-2.12; 3.10-2.12; 1.90-2.87; 4.29-2.87; 0.70-3.54; 3.10-3.54; 1.90-4.29; 4.29-4.29}
16	{0.62-0.62; 1.87-0.62; 3.12-0.62; 4.37-0.62; 0.62-1.87; 1.87-1.87; 3.12-1.87; 4.37-1.87; 0.62-3.12; 1.87-3.12; 3.12-3.12; 4.37-3.12; 0.62-4.37; 1.87-4.37; 3.12-4.37; 4.37-4.37}

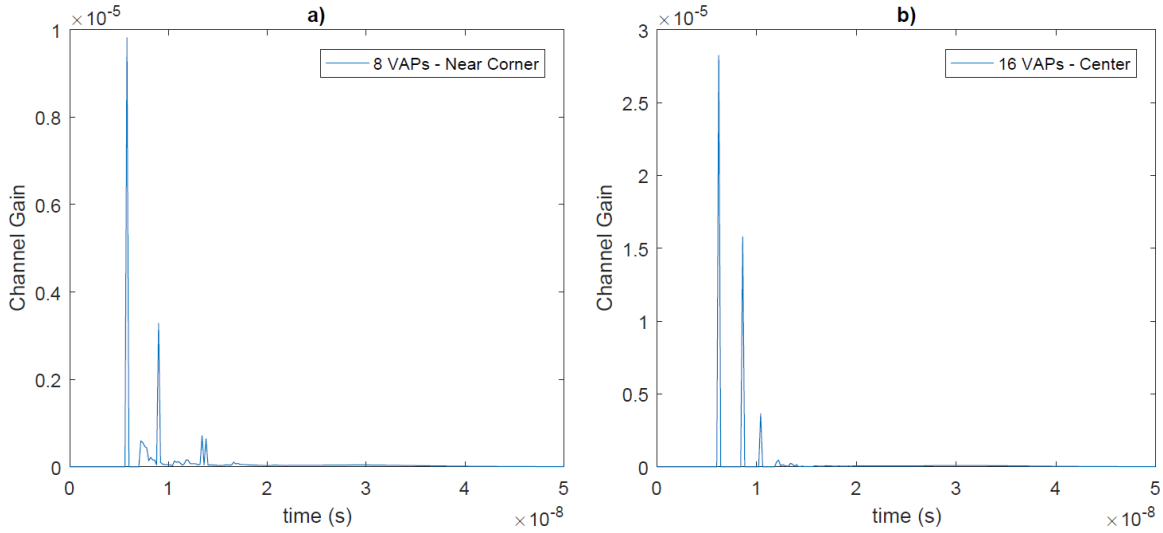

Figure 2. Power delay profile of the channel; a) 8 VAPs with receiver position close to the corner (0.5, 0.5, 0.85), a) 16 VAPs with receiver position at the center (2.5, 2.5, 0.85).

2.2. Optical Received Power

The schematic diagram of VLP system with four VAPs is given in Fig. 1. In our indoor scenario, LOS and NLOS link with three reflections are both considered for different numbers of Txs, specifically, N_t = 4, 5, 8, 9, 12 and 16. The respective channel coefficient of the optical links between the i^{th} VAP and the PD is represented by h_i. Thus, h_i is comprised of two components h_i^{LOS} and h_i^{NLOS} and given by,

$$h_i = h_i^{LOS} + h_i^{NLOS}, \tag{4}$$

Given that the LEDs have a Lambertian radiation pattern, h_i^{LOS} can be given as follows

$$h_i^{LOS} = \begin{cases} \dfrac{(m+1)A}{2\pi d_i^2}\cos^m(\alpha_i)\cos(\beta_i), & \left|\dfrac{\beta_i}{FOV}\right| \le 1, \\ 0, & otherwise, \end{cases} \tag{4a}$$

where m is the Lambertian emission order of planar LEDs, and depends on semi-angle at half power [19]. A is the effective area of the PD, d_i is the distance in meters between the i^{th} VAP and the PD, and FOV is the field of view of the PD. α_i denotes the angle of emergence measured from the Tx normal to the link between the i^{th} VAP and the PD. Similarly, β_i is the angle of incidence with respect to the PD normal. Since the normal vectors of VAPs and PD are parallel to each other, α_i is equal to β_i for the LOS link.

The indoor surfaces are generally *rough* relative to the wavelength of visible light, hence, most of the reflections of the VLP signals naturally have diffuse characteristics. We may assume that the reflective surfaces are divided into differential areas which also emit light intensity in a diffuse manner regardless of the angle of incidence. Therefore, we may say that each differential element has a Lambertian radiation pattern [24]. Then, the NLOS components from the i^{th} VAP with k bounces are given as follows

$$h_i^{NLOS(k)} = \begin{cases} L_i^{(1)} L_i^{(2)} \dots L_i^{(k+1)}, & \left|\dfrac{\beta_i^{(k+1)}}{FOV}\right| \le 1, \\ 0, & otherwise, \end{cases} \tag{4b}$$

where

$$\begin{aligned} L_i^{(1)} &= \frac{(m+1)dA}{2\pi d_{i(1)}^2}\cos^m\left(\alpha_i^{(1)}\right)\cos\left(\beta_i^{(1)}\right), \\ L_i^{(2)} &= \frac{dA}{\pi d_{i(2)}^2}\cos^m\left(\alpha_i^{(2)}\right)\cos\left(\beta_i^{(2)}\right)\rho_i^{(2)}, \\ L_i^{(k+1)} &= \frac{dA}{\pi d_{i(k+1)}^2}\cos^m\left(\alpha_i^{(k+1)}\right)\cos\left(\beta_i^{(k+1)}\right)\rho_i^{(k+1)}. \end{aligned} \tag{4c}$$

Here dA is the area of differential reflecting element. $d_{i(1)}$ is the link distance between i^{th} VAP and the first reflecting element. In a similar manner, $d_{(n+1)}$ is the link distance after n^{th} bounce where $n = \{1, 2, \dots, k\}$, in this study, $k = 3$. $\alpha_i^{(1)}$ and $\beta_i^{(1)}$ are the angle of

emergence from i^{th} VAP and the angle of incidence to the first reflecting element, respectively. Similar to the distances, $\alpha_i^{(n+1)}$ and $\beta_i^{(n+1)}$ denotes the angle of emergence and the angle of incidence after n^{th} bounce from i^{th} VAP, respectively. $\rho_i^{(n+1)}$ is the reflectivity coefficient of the n^{th} reflecting surface averaged over the visible light spectrum [24]. Then, the overall channel gain of the i^{th} VAP is given as

$$h_i = h_i^{LOS} + \sum_{n=1}^{k} h_i^{NLOS(n)}, \tag{5}$$

Since the effect of ISI is ignored, the intensity of light emitted during a symbol period is received within the same symbol interval. Therefore, the optical channel is comprised of intensity gathered in a symbol period regardless of time. Without loss of generality, the gain of the optical filter, $T_s(\beta)$, and the gain of the optical concentrator, $G(\beta)$, is assumed to be 1. Finally, the total optical received power is obtained as follows

$$P_r^o = \sum_{i=1}^{N_t} P_i^o \, h_i, \tag{6}$$

Optical power emitted from each LED, P_i^o, is 0.45 *W*. To make a fair comparison between indoor scenarios with different numbers of VAPs, the total power is kept constant. Therefore, the number of LEDs included in the VAPs depends on the number of VAPs considered. Table 2 exhibits the number of LEDs in VAPs, N_{led}, and the optical power of VAPs.

Table 2. VAP Parameters.

N_t	N_{led}	*VAP Power*	*Total Power*
4	*180*	*81 W*	*324 W*
5	*144*	*64.8 W*	
8	*90*	*40.5 W*	
9	*80*	*36 W*	
12	*60*	*27 W*	
16	*45*	*20.25 W*	

2.3. Horizontal Illuminance

For ergonomic lighting at the desk height in an office environment, it is necessary to achieve a certain illuminance which is 400 lux, minimally. The span of the illuminance in the whole room should be 200-800 lux, as well [23]. The homogeneity of lighting, on the other hand, is another important issue that is measured by the uniformity illuminance ratio (UIR). This parameter is described as the ratio of the minimum to the average illuminance. According to the lighting experts, the UIR should be over 0.7 [25].

The horizontal illuminance, I_h, is the amount of light hitting to the PD plane. By making use of the optical received power on the PD plane, I_h is defined as follows

$$I_h = \frac{P_r^o \kappa}{\mathrm{A}}, \tag{7}$$

where κ is the luminous efficacy depending on the light source efficiency. In this study, we consider typical off-the-shelf OSRAM LWG6CP LEDs with a luminous efficacy of 46 *lm/W* and a viewing angle of 120° at half power. Using an LED with a wide viewing angle is practical because it reduces the number of LEDs needed for room lighting [23].

2.4. RSSI-Based Positioning

This section evaluates the indoor positioning algorithm based on the RSSI and the trilateration method. By means of the CDMA decoder, the Rx unit separates the signal received from all VAPs with orthogonal codes, determines the location of the VAPs, and simultaneously measures the received electrical power from each VAP. The RSSI algorithm is, then, used to obtain at least three horizontal distances from the three known positions in the *xy*-plane, and by applying the trilateration method, the Rx position information is obtained.

2.4.1. Trilateration Method

The received electrical power from the i^{th} VAP, $P^e_{r(i)}$, can be given by

$$P^{\mathrm{e}}_{r(i)} = (P_i^o h_i^o R)^2, \tag{8}$$

where *R* denotes the PD responsivity. PDs used in optical communication are square-law devices; this means that the electrical power at the output of the detector is proportional to the square of the optical power at the input. This is due to the fact that for photons acting

on their active area, they generate a number of charge carrier proportional to the quantum efficiency. Thus the electrical current is proportional to the optical power. Naturally, electrical power is proportional to the square of optical power. From Eq. (8), it can easily be understood that $P^{e}_{r(i)}$ relates to the channel gain as well as the distance between VAPs and the Rx unit. Therefore, with the help of Eq. (4a) and Eq. (8), for the LOS link, the horizontal distance between the i^{th} VAP and Rx unit can be written as follows

$$d_i = \sqrt[(2m+6)]{\frac{\left(RP_i^o(m+1)Ad_h^{(m+1)}\right)^2}{4\pi^2 P^{e}_{r(i)}}}, \tag{9}$$

where d_h is the vertical distance between VAPs and the Rx plane, specifically, $d_h = 1.65\ m$. The position of Rx unit can be obtained by calculating the distances between the Rx unit and at least three projection positions of VAPs on the *xy*-plane. By means of the trilateration method, the distance equations can be given by [10]

$$\begin{aligned} d_1^2 &= (x_R - x_1)^2 + (y_R - y_1)^2 + (z_R - z_1)^2, \\ d_2^2 &= (x_R - x_2)^2 + (y_R - y_2)^2 + (z_R - z_2)^2, \\ d_3^2 &= (x_R - x_3)^2 + (y_R - y_3)^2 + (z_R - z_3)^2, \end{aligned} \tag{10}$$

where (x_R, y_R, z_R) is the coordinate of the Rx unit in three-dimensional space. Similarly, (x_i, y_i, z_i) is that of i^{th} VAP. Since the last terms at the right-hand sides of Eq. (10) are all the same, subtracting the second and third equations from the first one results in the following matrix form: [10]

$$\mathbf{b} = \mathbf{A}\mathbf{x}, \tag{11}$$

where

$$\begin{aligned} \mathbf{b} &= \frac{1}{2}\begin{bmatrix} d_1^2 - d_2^2 + x_2^2 + y_2^2 - x_1^2 - y_1^2 \\ d_1^2 - d_3^2 + x_3^2 + y_3^2 - x_1^2 - y_1^2 \end{bmatrix}, \\ \mathbf{A} &= \begin{bmatrix} x_2 - x_1 & y_2 - y_1 \\ x_3 - x_1 & y_3 - y_1 \end{bmatrix}, \quad \mathbf{x} = \begin{bmatrix} x_R \\ y_R \end{bmatrix}. \end{aligned} \tag{11a}$$

With the help of the linear least squares method, Eq. (11) can be solved $\hat{\mathbf{x}} = (\mathbf{A}^{\mathrm{T}}\mathbf{A})^{-1}\mathbf{A}^{T}\mathbf{b}$ [10]. The distance, d_i, is calculated over the received signal strength of the LOS link but the $P^{e}_{r(i)}$ includes AWGN noise as well as NLOS link contribution. Thus, the determined distance can not be the precise value of d_i. Finally, all system parameters considered in this study are summarized in Table 3.

Table 3. Parameters of The Considered VLP System.

Length of the room (X)	5 *m*
Width of the room (Y)	5 *m*
Height of the room (Z)	3 *m*
No. of Transmitters (N_t)	4, 5, 8, 9, 12, 16
LED distance from the ceiling	0.5 *m*
Elevation of the LEDs	-90°
Azimuth of the LEDs	0°
Semi-angle at half power ($\phi_{1/2}$)	60°
Lambertian order (m)	1
Power of the LED (P^{o}_{i})	0.45 $\sqrt{W}$
Luminous efficacy of the LED (κ)	46 *lm/W*
PD height from the floor	0.85 *m*
Elevation of the PD	90°
Azimuth of the PD	0°
Responsivity (R)	0.4 $A/\sqrt{W}$
Area of the PD (A)	0.0001 m^2
Field of view of the PD (FOV)	70°
Wall reflectivity coefficient (ρ_w)	0.8
Ceiling reflectivity coefficient (ρ_c)	0.5
Floor reflectivity coefficient (ρ_f)	0.3
Area of differential elements (dA)	0.04 m^2

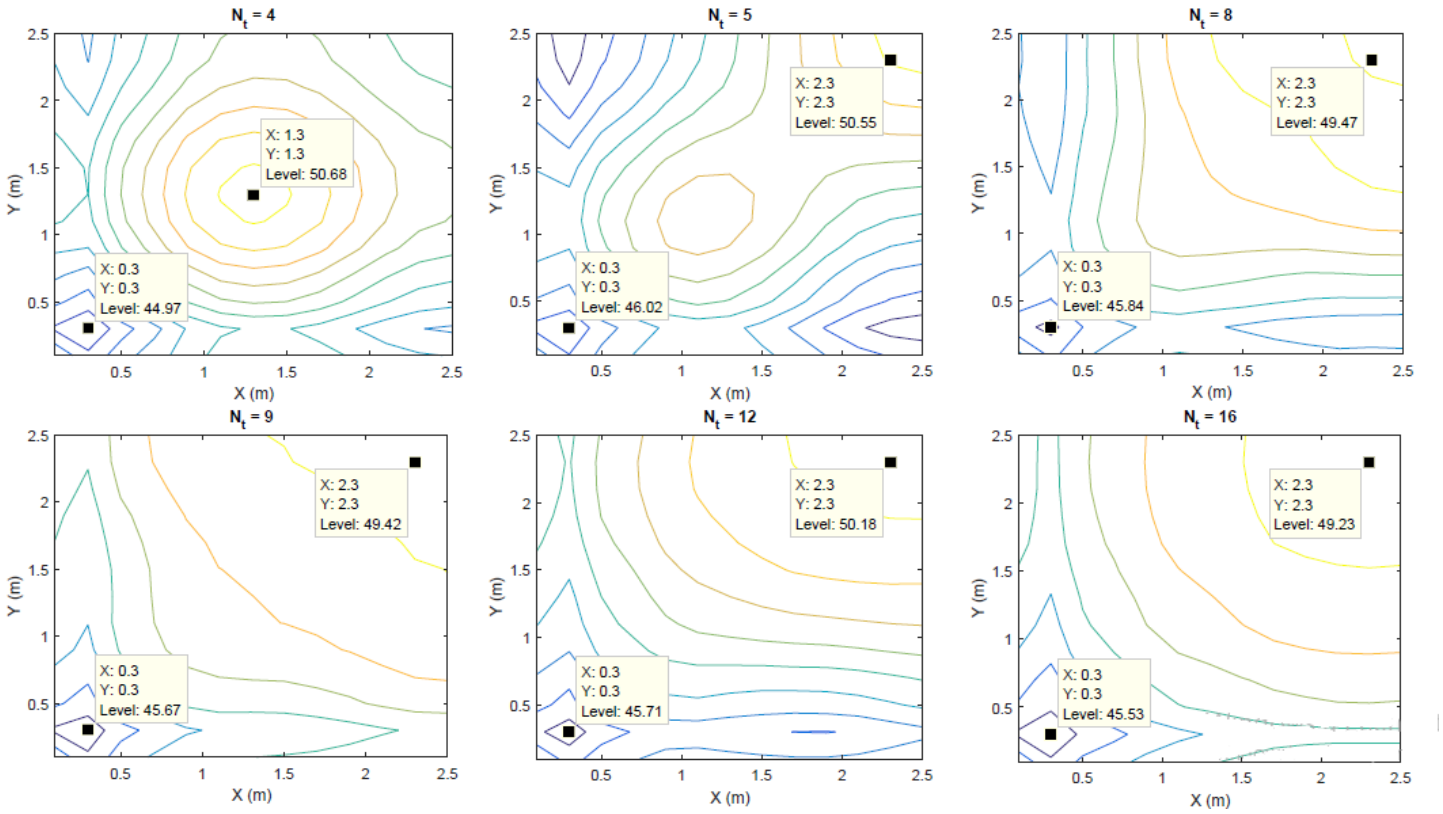

Figure 3. Overall link electrical SNR distribution for the RSSI based VLP with respect to different number of VAPs.

2.4.2. SNR Analysis

As the signal strength is highly sensitive to the indoor environment, the RSSI method is naturally sensitive to noise. Hence, to obtain realistic results noise in a VLP system should not be neglected. In our system model, Gaussian noise with a variance of σ^2 is considered as mentioned previously. Additionally, SNR is a crucial parameter for evaluating the performance of a VLP system. Then, the individual electrical SNR for the i^{th} VAP can be written as

$$SNR_i = \frac{P^{e}_{r(i)}}{\sigma^2}. \tag{12}$$

As stated in Section 2, the shot and thermal noises are both considered as additive noise sources. To calculate the variance of AWGN, the noise parameters in [26] are taken into consideration, and the noise power, which is equal to the σ^2 due to the zero mean, is calculated as $2.5\text{x}10^{-12}$ *W*. In the presence of AWGN, at least three distance estimates are required, among which the *longest* distance that causes the minimum individual SNR determines the VLP performance. To achieve acceptable distance error performance, therefore, the minimum individual SNR should be maximized. This is where the effect of LED deployment comes into play. Additionally, LED deployment also reduces the disruptive effect of NLOS components where reflections up to three bounces are considered here.

3. Results and Discussion

3.1. Simulation Results

In this section, the illuminance, SNR distribution and distance error performances with respect to the number of VAPs, N_t, are presented for the considered indoor scenarios. As exhibited in Table 2, to make a fair comparison for all cases, the optical power transmitted in a symbol period is assumed to be 324 W. In Table 4, the statistics of illuminance and received SNR, and also the mean square error (MSE) of distance are summarized according to the simulation results. It is worthy to note that the SNR given in the table is calculated via the electrical power, hence, we may say that the values regard to electrical SNR. Since the quarters of the room have the same electrical SNR distribution due to symmetry, only one quarter is shown in Fig. 3. The localization errors calculated as the Euclidean distance between the exact position and the estimated position obtained by the linear least squares algorithm are presented for the varying number of VAPs in Fig. 4.

The simulation results have shown that the cases for Nt = 5, 8, 9 and 16 are sufficient enough in terms of the UIR parameter since they both are greater than the proposed minimum value of 0.7. Furthermore, the best minimum SNR calculated in electrical manner is obtained for the case of Nt = 8 whereas maximum SNR is recorded for Nt = 5. The MSE of distance for Nt = 12 and 16 are the best, however, the scenario with 16 VAPs is preferable with a better UIR parameter. In terms of illumination, all the cases have the average illumination value which are more than 450 lux. I_h (%) corresponds to the percentage of the area with illuminance above 400 lux.

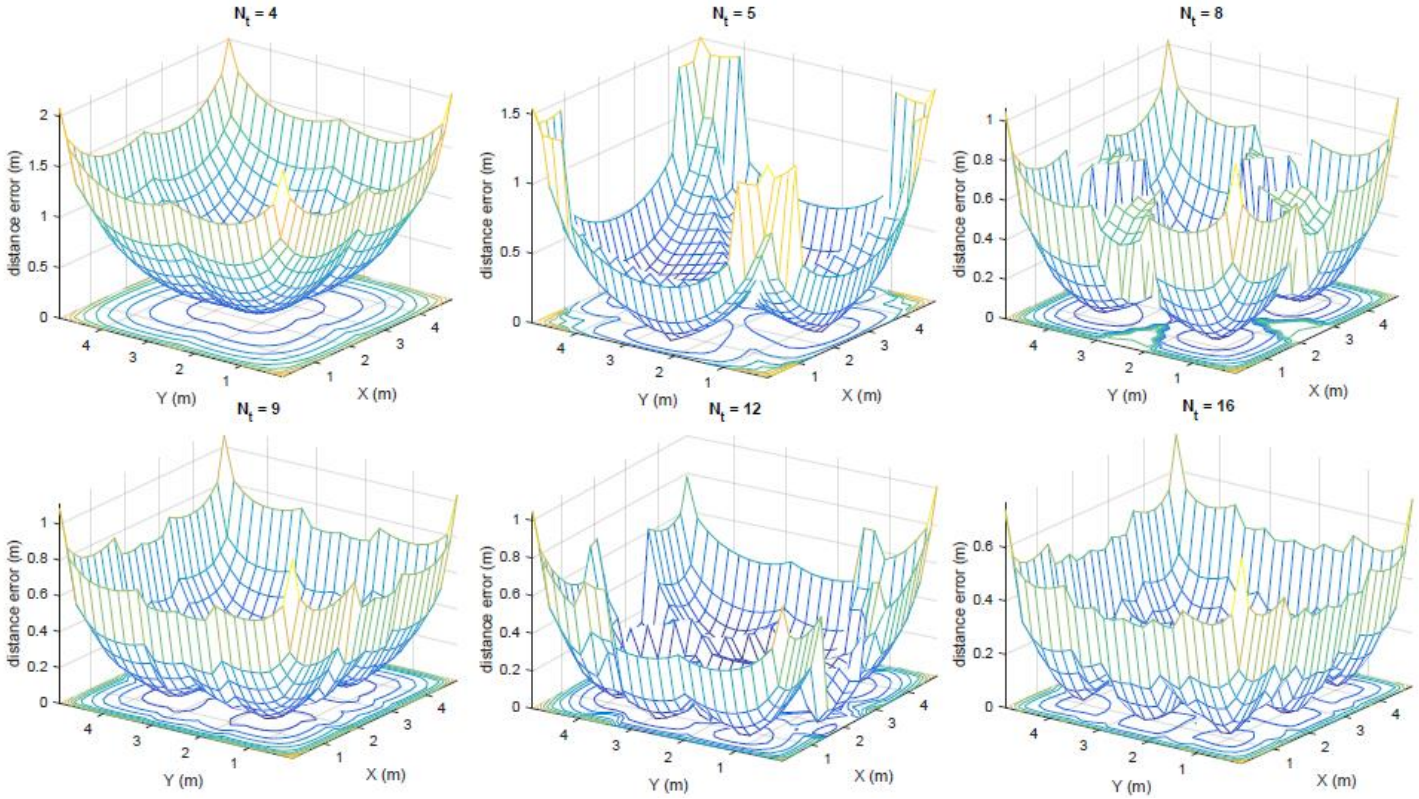

Figure 4. Distance error for the RSSI based VLP for different number of VAPs in the presence of NLOS link.

Table 4. Statistics of Illuminance, SNR Distribution, and MSE of Distance.

Overall Link	**Nt=4**	**Nt=5**	**Nt=8**	**Nt=9**	**Nt=12**	**Nt=16**
I_h (max), lux	622	627	554	542	589	526
I_h (min), lux	317	348	351	344	265	338
I_h (avg), lux	476	469	468	462	471	458
I_h (%)	88.4	85.2	88.4	92.6	83.6	89.7
UIR	0.66	0.74	0.74	0.74	0.56	0.73
SNR (max), dB	50.6	50.7	49.6	49.4	50.2	49.2
SNR (min), dB	44.8	45.6	45.7	45.5	43.2	45.4
d_{mse}, m	0.68	0.34	0.29	0.27	0.18	0.18

4. Conclusions and Recommendations

In this study, we have considered the effect of LED deployment with different number of VAPs, N_t, placed on the ceiling plane of a 2-D VLP system. The system is modeled mathematically utilizing the RSSI technique under the constraint of minimally 400 lux illumination at the desk height. As maximizing the individual SNR of each VAP increases the system performance of the whole VLP system, we aimed to obtain homogeneous illumination with the considered scenario. In this aspect, we have presented here the results of illumination, electrical SNR and also distance errors both evaluated with respect to N_t = 4, 5, 8, 9, 12 and 16. The simulation results have shown that the MSE of the distance is reduced with an increase in the number of VAPs. The MSE of distance for N_t = 12 and 16 are almost the same, however, the scenario with 16 VAPs is preferable with a better UIR parameter. As a conclusion, in this study, detailed results for system performances of six different VLP scenarios are presented. For future studies, it would be intriguing to investigate the effects of different parameters, such as FOV, on distance error performance with respect to LED deployment scenarios.

5. Acknowledge

This study was supported by Aksaray University Scientific Research Fund, grant number 2019-009.

References

[1] Do, T.-H. and Yoo, M. 2016. An in-depth survey of visible light communication based positioning systems, Sensors, 16, 5, pp. 1–40. https://doi.org/10.3390/s16050678

[2] Khan, L.U. 2017. Visible light communication: Applications, architecture, standardization and research challenges, Digital Communications and Networks, 3, 2, pp. 78–88. https://doi.org/10.1016/j.dcan.2016.07.004

[3] Tanaka, T. and Haruyama, S. 2009. New position detection method using image sensor and visible light LEDs, in Proc. IEEE 2nd Int. Conf., pp. 150–153, Dubai, United Arab Emirates. https://doi.org/10.1109/ICMV.2009.44

[4] Hann, S., Kim, J.-H., Jung, S.-Y., and Park, C.-S. 2010. White led ceiling lights positioning systems for optical wireless indoor applications, in Proc. 36th Eur. Conf. Exhib. Opt. Commun., pp. 1–3, Torino, Italy. https://doi.org/10.1109/ECOC.2010.5621490

[5] Lou, P., Zhang, H., Zhang, X., Yao, M. and Xu, Z. 2012. Fundamental analysis for indoor visible light positioning system, in Proc. 1st IEEE Int. Conf. Commun. China Workshops, pp. 59–63, Bejing, China. https://doi.org/10.1109/ICCCW.2012.6316475

[6] Lee, Y. U. and Kavehrad, M. 2012. Two hybrid positioning system design techniques with lighting LEDs and ad-hoc wireless network, IEEE Trans. Consumer Electron., 58, 4, pp. 1176–1184. https://doi.org/10.1109/TCE.2012.6414983

[7] Yasir, M., Ho, S.-W., and Vellambi, B. 2014. Indoor positioning system using visible light and accelerometer, J. Lightw. Technol., 32, 19, pp. 3306–3316. https://doi.org/10.1109/JLT.2014.2344772

[8] Hassan, N. U., Naeem, A., Pasha, M. A., Jadoon, T., and Yuen, C. 2015. Indoor positioning using visible LED lights: A survey," ACM Comput. Surveys, 48, 2, pp. 1–32. https://doi.org/10.1145/2835376

[9] Zhuang, Y., and et. al., 2018. A Survey of Positioning Systems Using Visible LED Lights, IEEE Comm. Surveys Tutorials, 20, 3, pp. 1963–1988. https://doi.org/10.1109/COMST.2018.2806558

[10] Hui, L., Darabi, H., Banerjee, P., and Jing, L. 2007. Survey of wireless indoor positioning techniques and systems, IEEE Trans. Syst., Man, Cybern., 37, 1, pp. 1067–1080. https://doi.org/10.1109/TSMCC.2007.905750

[11] Ziyan, J. 2012. A visible light communication based hybrid positioning method for wireless sensor network, in Second Int. Conf. on Intelligent System Design and Engineering Application (ISDEA), pp. 1367–1370, Sanya, Hainan, China. https://doi.org/10.1109/ISdea.2012.411

[12] Hyun-Seung K. and et al., 2013. An indoor visible light communication positioning system using a RF carrier allocation technique, J. Lightwave Technol., 31, pp. 134–144. https://doi.org/10.1109/JLT.2012.2225826

[13] Yang, S.-H., and et al., 2013. Indoor three-dimensional location estimation based on LED visible light communication, Electron. Lett., 49, 1, pp. 54–56. https://doi.org/10.1049/el.2012.3167

[14] Li, L., Hu, P., Peng, C., Shen, G., and Zhao, F. 2014. Epsilon: A visible light based positioning system, in Proc. 11th USENIX Symp. Netw. Syst. Design Implement. (NSDI), pp. 331–343, Seattle, WA, USA.

[15] Zhang, W., Chowdhury, M. I. S., and Kavehrad, M., 2014. Asynchronous indoor positioning system based on visible light communications," Opt. Eng., 53, 4, pp. 1–10. https://doi.org/10.1117/1.OE.53.4.045105

[16] Mohammed, N. A., and Elkarim, M. A. 2015. Exploring the effect of diffuse reflection on indoor localization systems based on RSSI-VLC, Opt. Exp., 23, 16, pp. 20297–20313. https://doi.org/10.1364/OE.23.020297

[17] Gu, W., Aminikashani, M., Deng, P., and Kavehrad, M. 2016. Impact of multipath reflections on the performance of indoor visible light positioning systems, J. Lightw. Technol., 34, 10, pp. 2578–2587. https://doi.org/10.1109/JLT.2016.2541659

[18] Tang, W., Zhang, J., Chen, B., Liu, Y., et. al, 2017. Analysis of indoor VLC positioning system with multiple reflections," in 16th Int. Conf. on Optical Comm. and Networks (ICOCN), pp. 1–3, Wuzhen, China. https://doi.org/10.1109/ICOCN.2017.8121297

[19] Mousa, F. I. K. and et. al,. 2018. Indoor visible light communication localization system utilizing received signal strength indication technique and trilateration method, Optical Engineering, 57, 1, pp. 1–10. https://doi.org/10.1117/1.OE.57.1.016107

[20] Xu, Y., and et. al., 2017. Accuracy analysis and improvement of visible light positioning based on VLC system using orthogonal frequency division multiple access, Optics Express, 25, 26, pp. 32618–32630. https://doi.org/10.1364/OE.25.032618

[21] Lausnay, S. D. and et al., 2015. Influence of MAI in a CDMA VLP system," in Proc. International Conference on Indoor Positioning and Indoor Navigation (IPIN), Banff, AB, Canada. https://doi.org/10.1109/IPIN.2015.7346949

[22] Qiu, Y., and et al., 2018. Visible Light Communications Based on CDMA Technology," IEEE Wireless Communications, 25, 2, pp. 178–185. https://doi.org/10.1109/MWC.2017.1700051

[23] Grubor, J., and et., al. 2008. Broadband Information Broadcasting Using LED-Based Interior Lighting, J. Lightw. Technol., 26, 24, pp. 3883–3892. https://doi.org/10.1109/JLT.2008.928525

[24] Lee, K., Park, H., and Barry, J. 2011. Indoor Channel Characteristics for Visible Light Communications, IEEE Commun. Lett., 15, 2, pp. 217–219. https://doi.org/10.1109/LCOMM.2011.010411.101945

[25] Ding, J.P. and Ji, Y.F. 2012. Evolutionary algorithm-based optimisation of the signal-to-noise ratio for indoor visible-light communication utilising white light-emitting diode, IET Optoelectronics, 6, 6, pp. 307–317. https://doi.org/10.1049/iet-opt.2012.0044

[26] Xueli, Z., Jingyuan, D., Yuegang, F., and Ancun, S. 2014. Theoretical accuracy analysis of indoor visible light communication positioning system based on received signal strength indicator, J. Lightwave Technol., 32, 21, pp. 4180–4186. https://doi.org/10.1109/JLT.2014.2349530